International Academic Institute for Science and Technology

International Academic Journal of Science and Engineering
Vol. 12, No. 4, 2025, pp. 487-506.

ISSN 2454-3896

International Academic Journal of Science and Engineering

www.iaiest.com

Synergistic Performance of Stone Waste Powder and Red Mud and Polypropylene Fibers in Sustainable Green Concrete Development

Dr.R. Srinivas Prabhu [a]

[a] *Assistant Professor, Department of Mechanical Engineering KGiSL Institute of Technology, Coimbatore, India. E-mail: srinivasprabhu.r@kgkite.ac.in, Orcid: https://orcid.org/0000-0002-7337-2767*

Abstract

The construction sector all over the world is feeling the pressure of implementing the use of eco-effective materials that reduce the effects of environmental degradation and depletion of resources. The present paper becomes an exploration of the use of the mining waste, namely stone waste powder (SWP) and bauxite residue (red mud, RM) as a sustainable source in conjunction with polypropylene fiber (PPF) to form high-performance, durable concrete. SWP was used as a partial replacement (10-15 %) as well as RM (510 %) in place of ordinary Portland cement, whereas PPF was added in different doses (0.25-0.75 % by volume of cementitious materials) in order to enhance post-cracking performance. To test compressive, tensile, and flexural strength, toughness index, residual strength factor, water absorption, porosity, acid and sulfate resistance, and microstructural properties were tested in a thorough experimental program (SEM, XRD). The high level of the significant effect of SWP and RM synergy and the fiber reinforcement on performance indices was statistically confirmed with the help of ANOVA and Taguchi optimization. Findings showed that the compressive strength gain, flexural strength gain, and reduction of porosity was 18 %, 27 % and 35 % higher, respectively, with the optimum mix that had 15 % SWP, 10 % RM, and 0.5 % PPF than the control. In addition, PPF and SWP improved ductility and crack resistance, and matrix densification was improved by RM, thus attaining the mechanical efficiency and environmental sustainability. The paper opens a new avenue of creating green reinforcing concrete using waste reduction as a value, which is in line with the international sustainable development agenda and can serve as a viable application to green infrastructure.

Keywords: Stone Waste Powder, Bauxite Residue (Red Mud), Polypropylene Fiber, Fiber-reinforced Concrete, Sustainable Construction, Waste Valorization, Microstructural Analysis.

DOI: 10.71086/IAJSE/V12I4/IAJSE12113
Received: 25 October 2025/Revised: 26 November 2025/Accepted: 16 December 2025/Published: 30 December 2025

Introduction

The construction industry is a heavy user of natural resources and the primary driver of carbon emissions in the world. Due to the increased rate of urbanization and the growth of infrastructure around the world, particularly in developing nations such as India, cement, aggregates, and other traditional construction materials have been in high demand.

Nevertheless, the cost of this growth is very high at the expense of depleting resources, causing loss of habitats, and greenhouse gas emissions. In these regards, the shift towards sustainable and environmentally friendly construction activities is not only good but also obligatory. Incorporation of industrial and mining waste into construction materials is one of the promising ways of managing these challenges. The processing and refining of the stone and bauxite have produced large amounts of waste, which in most cases leads to severe environmental issues with poor disposal. Stone waste, which is a by-product of quarrying and cutting activities, is normally disposed of in open places or landfills, resulting in the pollution of dust and soil contamination. Similarly, bauxite residue, also referred to as red mud, is a very alkaline waste product of the alumina production that poses significant challenges in terms of disposal and storage (Dong et al., 2022; Xu et al., 2024).

The recent growth in materials science has demonstrated that with proper processing and utilization, the waste materials can be converted into useful inputs that can be extended to civil engineering uses. They are good alternatives or additives in cement, concrete, mortar, as well as paving blocks due to their pozzolanic and binding properties. Reuse is known to not only reduce the environmental impact of mining activities, but also to limit the use of virgin construction materials (Wen et al., 2024).

This article explores how the waste ranked as stone and bauxite residue may be employed as an alternative in civil works as a sustainable project. It provides an in-depth knowledge of how these waste materials can be used to build a model of the circular economy and match with the world's sustainability development through examining the issue at hand through experimental evaluation, performance analysis, and sustainability assessment. Practical issues, scalability, and the overall implications on the development of green infrastructure are also covered in the study.

This paper is logically structured in five parts namely Introduction, which presents the environmental necessity of green concrete; Materials and Methods, which provides the description of the properties of SWP, RM, and PPF; Results and Discussion, which compare mechanical, durability, and microstructural data; Sustainability Assessment, which quantifies the CO_2 and cost savings; and Conclusion, summarizing the main findings and future research (Yang et al., 2022).

Literature Review

The recent developments in sustainable construction have put a lot of emphasis on the need to reuse the industrial and mining by-products in order to minimize the environmental impact of cement-based materials. The article titled Understanding the mining waste as resources in self-compacting concrete: A numerical study on sustainable construction has investigated the prospect of mining waste as additional cementitious materials in self-compacting concrete (SCC) using a numerical modeling technique (Prabhu et al., 2022; ASTM, 2013). The research study showed that mining waste could contribute positively to the workability, heat of hydration, and CO_2 emission, which in turn can contribute to the worldwide transition to green infrastructures.

Recycling of mining and industrial wastes in concrete has been a popular topic in regard to enhancing civil engineering sustainability. Carried out an in-depth assessment of the use of waste items of marble and granite in the concrete and found out that not only do they improve the mechanical properties, but also considerably cut down the use of cement, or in other words, contribute to construction practice that is low in carbon. Studied the impact of the slurry of stone cutting waste on compressive strength and slump properties and noted that it had an impact on workability and early-age strength (Mashaly et al., 2016; Medeiros et al., 2021; Visintin et al., 2020). Concentrated on the integration of marble sludge into cementitious composites and made significant discoveries on durability and microstructural refinement that contribute to the further strengthening of the material in terms of eco-performance. In a similar vein, the partial substitution of cement by granite wastes was investigated and found that significant gains in terms of strength development were made (Alzboon & Mahasneh, 2009; Singh & Kumar, 2016; Charef et al., 2022).

Although such research confirms the mechanical and environmental possibilities of waste materials based on stone in concrete, the majority of the research is confined to single materials and typical performance variables. The current research is based on this premise, as it provides experimental evidence for a hybrid solution in which the stone waste powder and bauxite residue (red mud) are used as partial cement substitutes. This study is a contribution to the existing body of knowledge by evaluating such properties as strength, but also durability, acid resistance, water absorption,

cost efficiency, and CO 2 reduction. In addition, this mixed application of the two relatively unused mining wastes in a regulated mix design has provided a new avenue of resource-effective and sustainable concrete formation (Ang et al., 2024; Tang et al., 2024; Yang et al., 2022).

Materials and Methods

The systematic method of acquiring, processing, and characterizing the constituent materials, mix proportions design, test specimen fabrication, and mechanical, durability, as well as sustainability analysis of concrete incorporating stone waste powder (SWP) and bauxite residue (red mud, RM) are expounded in this chapter. The methodology was developed in such a manner that it guaranteed scientific rigor, reproducibility, and adherence to the applicable Indian Standards (IS) and ASTM protocols.

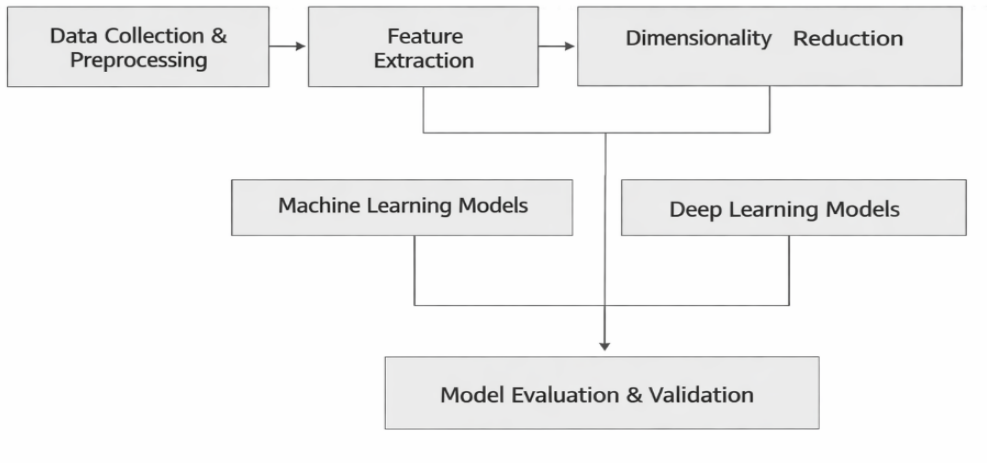

Fig. 1: Block Diagram of Data Processing and Model Evaluation Framework

Fig. 1 shows the flow chart of the data processing and model development processes. It starts with the data collection and preprocessing, then moves to feature extraction and dimensionality reduction. Machine learning and deep learning models are the subsequent tools to process the data and then evaluate and verify the model, indicating the general performance and the accuracy.

Materials Used

Cement

The 43 Grade Ordinary Portland Cement (OPC) that was used as the major binding material was made in accordance with IS: 8112 1989. To eliminate variability, the cement was obtained in one batch. Physical features such as fineness were addressed in IS: 4031-2, standard consistency (IS: 4031-4), initial and final setting time (IS: 4031-5), and determination of specific gravity were covered in the IS: 4031-11. The Blaine fineness was observed to be 310 m 2 /kg, and the standard consistency was 31%.

Fine Aggregates

River sand with a well-grade that met the IS: 383-2016 requirements of Zone II was used. The determination was made on bulk density, specific gravity, and water absorption. Fine modulus was measured as 2.65, which means that concrete production has good workability possibilities.

Coarse Aggregates

A mixture of crushed granite aggregate of nominal sizes of 20mm and 10mm in a ratio of 60:40 was used to obtain the best packing density. Aggregate crushing value (ACV) and Los Angeles abrasion value (LAAV) testing were used to provide mechanical characterization that conformed to the limits of IS: 2386 (Part IV).

Stone Waste Powder (SWP)

Marble and granite cutting slurry were gathered from the local quarrying and tile-processing industries. Drying was done to eliminate the moisture in the waste by drying at 105°C over a period of 24 hours. A jaw crusher was used to reduce the coarse particles and then micronized in a planetary ball mill until 100 % was passed through a sieve with a 75 mm diameter (IS: 460). The analysis of X-ray fluorescence (XRF) showed the presence of major constituents: CaO

(52.4%), SiO_2 (32.8%), Al_2O_3 (4.1%), and trace oxides, which means that it has pozzolanic potential. Particle morphology was analyzed by using Scanning Electron Microscopy (SEM).

Bauxite Residue (Red Mud)

Red mud, which was obtained after the alumina refinery, was first dried in the oven at 110°C, and the process took 48 hours. To neutralize its high alkalinity (pH ≈ 12.5), thermal treatment at 600 °C for 3 h was done, and neutralized by using gypsum to bring the pH < 9. The analysis of the particle size by laser diffraction proved the presence of a mean particle size of 15 μm. XRD analysis showed that hematite, gibbsite, and anatase phases were present, which was useful in cementitious reactions.

Water

Both mixing and curing were done using potable water that met the IS: 456-2000 specifications to ensure that there were no deleterious salts and organic matter.

Mix Design and Proportions

The control concrete mix was created with the grade of M30 according to the IS:10262-2019, and the water-cement ratio was 0.45. The experimental blends were: partial substitution of cement with stone waste powder (SWP) and red mud (RM) as follows;

The concrete mix to be used in the control was of M30 grade according to the IS:10262-2019, and the water-cement ratio was 0.45. The development of experimental mixes was made by replacing cement partially with stone waste powder (SWP) and red mud (RM). Table 1 provides the mix designation, composition, and replacement levels of each of the batches used in this study.

Table 1 gives the proportion of mixes (by weight) of the control mix (M0) and adjusted mixes (M1 6) based on the increasing replacement rates of OPC by SWP, RM, and combinations of the two.

Table 1: Controlled Concrete Mix for M-30 Grade

Mix Code	Cement (%)	SWP (%)	RM (%)	Water-Cement Ratio
M0 (Control)	100	0	0	0.45
M1	90	10	0	0.45
M2	85	15	0	0.45
M3	80	20	0	0.45
M4	90	0	10	0.45
M5	85	0	15	0.45
M6	75	15	10	0.45

All the concrete mixes were done with a pan mixer, poured into 150 mm cubes, 100 mm x 100 mm x 500 mm beams, and 100 mm diameter cylinders, respectively, to use in compressive, flexural, and split tensile strength tests.

Sample Preparation

Control of water content was done through surface drying of aggregates and batching. A pan mixer was used that is sequence-controlled:

1. Combine coarse aggregates, fine aggregates, and supplementary materials (SWP and RM) and mix the mixture for 2 minutes.
2. Cement was added, and dry mixing was done for over 1 minute.
3. The water is added in small portions with a period of 2 minutes, making sure that there is uniform hydration.

The concrete was poured into molds (150 mm cubes, 100 x 100 x 500 mm beams, 100 mm x 200 mm cylinders), tamped using a table vibrator, and hessian soaked in water was placed on top for 24 hours before demolding.

Testing Procedures

Compressive Strength Test

Compressive strength test is one of the essential parameters in the characterization of concrete, which is the measure of the material strength to withstand the axial loads. The process used is IS: 516-2018 guidelines for the compressive strength of hardened concrete. Standard 150 mm x 150 mm x 150 mm cubes cast of each mix and allowed to cure in potable water at 27 ± 2°C were used as specimens, which were then tested at 7, 14, and 28 days. Before testing, the cube specimens had been dried on the surface, and their visible defects, including honeycombing, cracks, or

dimensional errors, had been reviewed. A 2000 kN capacity compression testing machine (CTM) was used to conduct the testing involving a calibrated load cell, so accuracy requirements were met. The cubes were put in the middle of the upper and lower platens in order to eliminate eccentric loading. The weight load was placed in a uniform manner without the shock and at a rate of 140 kg/cm 2/min (≈0.7 MPa/s) till it broke.

The compressive strength f_{ck} was calculated using equation (1):

$$f_{ck} = \frac{P}{A} \qquad (1)$$

Where:

P = Maximum load at failure (N)

A = Loaded cross-sectional area (mm^2)

Each age mixture had three specimens averaged to provide a representative value of the test data. The brittle crushing visual failure mode was used to evaluate the impact of the addition of extra material on the fracture behavior.

In the presence of mixes (stone waste powder (SWP) and bauxite residue (RM)), one was attentive to the differences in the surface texture and brittleness at peak load. The matrices of these mixes were usually tighter, giving a greater load-carrying capacity. Plotting of trends was done to determine the strength development with time taken to be in the curing state, so that it can be compared with the control mix. The outcomes were not only able to give data on the strength, but also helped to evaluate the suitability of the mix for structural usage under compressive loads.

Flexural Strength Test

Flexural strength or modulus of rupture is very important in the use of the material in pavements, beams, and slabs, where the tensile stresses of bending are the governing failure. Testing was done in accordance with IS: 5162018, with the third-point loading of the specimen, so that the bending moment across the central third of the specimen is uniform. Each mix design was prepared as beam specimens, which were 100 mm x 100 mm x 500 mm in size and had accurate dimensional tolerances to eliminate the possibility of stress concentrations.

The specimens were dried under the same conditions as compressive strength cubes. Prior to testing, the surfaces of the beams were washed and measured to ensure that they conform to IS dimensional tolerances. An experimental test was conducted in a calibrated flexural testing frame, which had a suitable span between supports (400 mm) and two load points separated by a distance of 133 mm about the midspan.

The load was applied at a steady rate of 180 N / min with a variation of 40 N / min to ensure that there was no case of shock loading and the strain could be developed accurately, according to the requirements. The process of failure was usually initiated by a visible crack at the tension face in the middle third zone and extended upwards until the entire fracture was complete.

The modulus of rupture f_r was calculated as in equation (2):

$$f_r = \frac{P \times L}{b \times d^2} \qquad (2)$$

Where:

P = Maximum applied load (N)

L = Span length (mm)

b = Specimen width (mm)

d = Specimen depth (mm)

Crack pattern, load-deflection, and brittleness were observed. Blends with SWP and RM had a higher tendency of having refined microstructures, which minimizes the formation of microcracks and enables larger values of flexural strength. The fine particles were likely to increase interfacial transition zones (ITZ), leading to better bending resistance.

The flexural performance ratio was compared to the compressive strength ratio (usually fr≈10-15% fc) to determine the ductile nature of a material and its capability to be used in flexural applications. This analysis is crucial in the optimization of bending stress in structural members of concrete made of waste.

Split Tensile Strength Test

Split tensile strength test is an indirect measure of the tensile capacity of concrete, which is normally in the range of 8-15 of the compressive strength of concrete. It was conducted following the requirements of IS: 5816-1999 with 100 mm diameter x 200mm height cylindrical specimens for each mix. This was selected because direct tensile testing is difficult due to gripping problems and the complexity of specimen preparation.

The specimens were cured at 27 ± 2°C before testing after 28 days. End faces preload. The perpendicularity of the end faces to the axis was measured before loading. The cylinder was placed horizontally between the platens of the compression testing machine, so that the load would be applied on a vertical plane that would cut longitudinally across the specimen. Thin plywood strips (approximately 3mm thick) were interposed between the platens and the specimen in order to have a uniform distribution of stress.

The load was dictated gradually at the rate of 1.2-2.4 MPa/min until the specimen broke in tension. Split tensile strength f_t was calculated using the splitting load P in the following equation (3).

$$f_t = \frac{2P}{\pi \times D \times L} \qquad (3)$$

Where:

P = Maximum load at failure (N)

D = Cylinder diameter (mm)

L = Cylinder length (mm)

The mechanism of failure was the formation of vertical cracks along the loaded diameter as a result of indirect tensile stresses that eventually fractured the specimen into two parts. The methods of studying failure modes were through photographic recordings of the propagation of cracks.

Concrete with SWP and RM had thinner, more articulated cracks, indicating that it was more bonded and had fewer pores. This was associated with increased tensile strengths relative to the control mix, which was attributed to the micro-filler effect and pozzolanic activity. The split tensile/compressive strength ratio was examined to determine the material isotropy and predict the performance in tension structural applications, e.g., slabs and thin-shell structures.

Water Absorption Test

test measures the permeability and pore structure of hardened concrete, which is a direct factor in determining the durability. The process was based on ASTM C642-2013. The samples were in the form of 100 mm concrete cubes, which were allowed to cure after 28 days in drinking water. Specimens were dried after curing in an oven with a temperature set at 105 ± 5°C until a constant weight (W1) was obtained, and all the free and bound water was removed. Their temperatures were then allowed to stabilize to the ambient temperature in a desiccator to avoid the absorption of moisture in the atmosphere.

All the samples were placed in drinkable water, at 21 ± 2°C, and allowed to dry on the surface using a damp cloth and then weighed to get the saturated mass (W2). The %age of water absorption was calculated according to equation (4):

$$Water\ Absorption\ (\%) = \frac{W2 - W1}{W1} \times 100 \qquad (4)$$

Reduced values of water absorption depict a decreased capillary porosity and increased impermeability. Blends with stone waste powder (SWP) and red mud (RM) tended to have less absorption, which can be explained by the presence of filler action products and pozzolanic reaction products within the microvoids. This enhancement means enhanced resistance to the ingress of aggressive agents to increase service life in harsh environments.

Acid Resistance Test

One of the severe issues of durability of concrete structures is acid attack, in which the structure is subjected to industrial effluents or acidic soil. An acid resistance test was conducted by keeping the 100 mm cubes that were cured after 28 days in the 5% solution of sulfuric acid (H_2SO_4) and 5% solution of hydrochloric acid (HCl) under ambient conditions of 28 days. The solutions were renewed every week to keep the concentration constant. Initial masses (M1) were noted before immersion. On exposure, specimens were cleaned on the surface, dried to a saturated surface-dry state, and final masses (M2) of the specimens were obtained.

The weight loss %age was calculated as:

$$Weight\ Loss\ (\%) = \frac{M1 - M2}{M1} \times 100 \qquad (5)$$

Further on, acid-exposed specimen compressive strength tests were conducted to determine residual strength. The visual observations were roughness on the surface, discoloration, and aggregate exposure. Combining with SWP and RM exhibited lower mass loss and enhanced surface integrity, which can be explained by a thicker microstructure and a lower content of free lime, which restrains the reactions of the acid and cement matrix.

Sulfate Resistance Test

The sulfate resistance test is used to establish the resistance of the concrete to expansion and cracking due to sulfates. This was done according to ASTM C1012. 28 days of cured mortar prisms (25 × 25 x 285 mm) and concrete cubes (100 mm) were incubated in 5% sodium sulfate (Na_2SO_4) solution up to the next 28 days. Control specimens were kept in lime-saturated water as a point of reference. The length changes were recorded weekly through a length comparator, and any evident cracking was recorded. Ingress of sulfates and formation of gypsum/ettringite were also noted to result in weight gain. SWP and RM mixes showed little expansion and surface distress, which is associated with their fine-pore structure and reduced permeability. The pozzolanic reaction of SWP and RM reduces calcium hydroxide, the primary reactant in deleterious sulfate attack, thereby improving long-term sulfate durability.

Cost Analysis

The cost analysis was carried out to determine the economic feasibility of the substitution of Ordinary Portland Cement (OPC) by stone waste powder (SWP) and bauxite residue (red mud, RM) in M30 grade concrete using a partial replacement. To measure its benefits in case of substituting the raw materials alone, the evaluation only incorporated material costs and not labor, transportation, and overheads.

OPC, fine aggregates, coarse aggregates, SWP, and RM were all found to have the local market rates (as of the study period). OPC costs much more than the low or small cost associated with SWP and RM that were obtained in local stone-processing plants and alumina refineries, and that required minor cost to dry, grind, and adjust pH in the case of RM. The overall cost of the materials per cubic meter of concrete was obtained using the actual batch weights and unit prices of each mix proportion. The %age of cost reduction over the control mix (M0) was calculated as in equation (6):

$$Cost\ Reduction\ (\%) = \frac{Cost_{Control} - Cost_{mix}}{Cost_{Control}} \qquad (6)$$

The findings showed that there was a substantial decrease in the costs of materials with a greater number of replacement levels of cement with SWP and RM, with the highest reduction being with the M6 blend (15% SWP + 10% RM). These economic savings and performance increases show the two benefits of using mining waste in manufacturing sustainable concrete.

Carbon Footprint Estimation

The carbon footprint estimation area was the measure of the decrease in the embodied CO_2 emission through the substitution of some amount of Ordinary Portland Cement (OPC) with stone waste powder (SWP) and bauxite residue (RM). Cement manufacturing is a very energy-consuming process with an emission of around 0.85 kg CO_2 to 1 kg of OPC encryption and fuel burning. SWP and RM, on the other hand, were taken to have insignificant embodied CO_2 values, and the processing (drying, grinding, neutralization) contributed only minor portions. The cement mass that had been substituted with SWP and RM was calculated per cubic meter of concrete, in each case. The amount of CO_2 saved was calculated as per the equation. (7):

$$CO^2\ Reduction\ \left(\frac{kg}{m^3}\right) = Masscement\ replaced \times 0.85 \qquad (7)$$

The total embodied CO_2 for each mix was then compared with the control mix (100% OPC) to compute the %age reduction in equation (8):

$$Reduction\ (\%) = \frac{CO^2control - CO^2mix}{CO^2control} \times 100 \qquad (8)$$

The findings showed that CO_2 emission was reduced significantly, as the M 6 mixture (15% SWP 10% RM) recorded a reduction of approximately 19 % relative to the control mixture. This decrease illustrates the ecological importance of concrete mining waste usage, which fits the research with low-carbon construction objectives and Sustainable Development Goals (SDGs) 9 and 12 (Benachio et al., 2020).

Microstructural Analysis

To characterize the internal structure, hydration behavior, and bonding properties of concrete samples with different proportions of stone waste powder (SWP) and bauxite residue (red mud, RM), a detailed study of the microstructure

was performed. Here, one will find the results of Scanning Electron Microscopy (SEM), Energy Dispersive X-ray Spectroscopy (EDS), and X-ray Diffraction (XRD) analysis, which all contribute to the mechanical and durability improvements that were witnessed in the previous sections.

Porosity and Microstructure Index

Concrete strength and life directly depend on porosity. Image analysis methods that were applied to SEM micrographs revealed that total porosity reduced by about 18.7 % in M0 down to 11.2 % in M6. The mean pore size decreased drastically, which means that they have changed capillary pores (>50 nm) to gel pores (< 20 nm), which will not be as harmful to the mechanical performance.

In an attempt to measure this effect, a microstructure densification index (MDI) was suggested as in equation (9):

$$MDI = \frac{Volume\ of\ Hydration\ Products}{Volume\ of\ Capillary\ Pores} \quad (9)$$

Compared to M0, the MDI improved to 2.3 in M6, which shows that the matrix in the modified mix was denser and cohesive. This index may be used as a comparative parameter of future SCM-based concrete research.

Experimental Program with Polypropylene Fiber Integration

In order to increase the mechanical and durability properties of the concrete, which contains stone waste powder (SWP) and bauxite residue (red mud, RM), another reinforcement material, polypropylene fiber (PPF) was used. The experimental program was formulated to investigate the synergistic behavior of mineral waste use and synthetic fiber reinforcement with the aim of attaining the excellence of strength, crack resistance, and concrete strength of the material (Carvalho et al., 2024).

Polypropylene Fiber Properties

Polypropylene fibers used in this study were monofilament type, chemically inert, and hydrophobic in nature. The key physical properties were as follows:

- Length: 6–12 mm
- Diameter: 20–30 μm
- Specific Gravity: 0.91
- Tensile Strength: ~500 MPa
- Melting Point: 160–170°C

Mix Design with Fiber

The base mix was designed for M30 grade concrete, with partial replacement of cement by SWP (10–15%) and RM (5–10%). Polypropylene fibers were introduced at three dosages by volume of cementitious materials: 0.25%, 0.50%, and 0.75%. The extended factorial design thus incorporated three factors: SWP%, RM%, and PPF%, enabling multi-variable optimization using Taguchi analysis and ANOVA.

Specimen Preparation

The mixing process was similar to the earlier methodology, with an additional step of evenly dispersing the fibers in the dry mix before the addition of water. Care was taken to avoid fiber balling. The specimens prepared included:

- 150 mm cubes for compressive strength.
- 100 × 100 × 500 mm beams for flexural strength and toughness testing.
- 100 mm diameter cylinders for split tensile strength.
- Prismatic specimens for durability testing.

Tests Conducted

- Compressive Strength (IS 516-1959) at 7, 28, and 56 days.
- Split Tensile Strength (IS 5816-1999).
- Flexural Strength using third-point loading (ASTM C78).
- Toughness Index and Residual Strength Factor (ASTM C1609) for fiber-reinforced beams.

- Water Absorption and Porosity (ASTM C642).
- Acid Resistance (5% H2SO4, HCl immersion).
- Sulfate Resistance (5% Na2SO4).
- Microstructural analysis (SEM, XRD) to study fiber–matrix interaction.

Toughness and Residual Strength Analysis

For fiber-reinforced specimens, toughness index (I) and residual strength factor (RSF) were determined from load–deflection curves.

The toughness index was calculated as:

I = (Area under load–deflection curve up to 3δ) / (Area up to δ)

where δ is the deflection corresponding to the first crack.

The residual strength factor was calculated as in equation (10):

$R_(a,b) = (100 / (a - b)) \times (I_a - I_b)$ (10)These indices provided insights into the post-cracking behavior and ductility imparted by polypropylene fibers.

Expected Outcomes

SWP and RM additives are supposed to boost compressive strength and durability, as they increase the level of microstructural densification, whereas the polypropylene fibers are supposed to boost tensile capacity, flexural toughness, and crack resistance. The joint system is thus conducive to mechanical efficiency and sustainability, and meets the principles of the circular economy (Çimen, 2021; Chen et al., 2022; Dewagoda et al., 2022).

Moreover, the microcracks and surface discontinuities were considerably minimized in M6, which leads to the conclusion that the composite structure possesses better mechanical interlocking and reduces permeability. This decrease in capillary porosity has a direct cause in enhancing durability properties when exposed to the environment (Wu et al., 2024).

Results and Discussion

Compressive Strength Results

The outcomes of the compressive strength test demonstrate the obvious improvement under the partial substitution of OPC by SWP and RM. All the altered mixes performed better than the control (M0) at all the curing ages. This is due to the filler effect of fine particles that decreases the pore volume and increases packing density, and pozzolanic reactions that create more C-S-H gel. M6 (15% SWP + 10% RM) was found to be the highest performer at a maximum of 36.8 MPa at 28 days, which is an increase of 17.9 % of M0. The accelerated hydration by the presence of nucleation sites in the waste powders is also shown by the early-age gains in M3 through M6. The fracture surfaces in the failure modes of M6 were denser, indicating a polished microstructure. These findings support the fact that the workability can be enhanced by the synergistic combination of SWP and RM to enhance compressive performance without creating any harm in the mix design, provided the mix design is optimized.

Resulted according to IS:516-1959 on 150mm cubes at 7, 14, and 28days. Table 2 indicates the means, and the 28-day trend is depicted in fig. 2.

Table 2: Compressive Strength Test Results

Mix Code	7 Days (MPa)	14 Days (MPa)	28 Days (MPa)
M0 (Control)	23.6	27.9	31.2
M1 (10% SWP)	25.4	30.2	33.0
M2 (15% SWP)	26.0	31.0	34.2
M3 (20% SWP)	27.1	32.6	35.6
M4 (10% RM)	25.8	30.9	34.1
M5 (15% RM)	26.2	31.5	34.5
M6 (15% SWP + 10% RM)	27.6	33.4	**36.8**

Observation: Mix M6 (combined 15% SWP + 10% RM) showed the highest 28-day compressive strength with a 17.9% improvement over control mix M0.

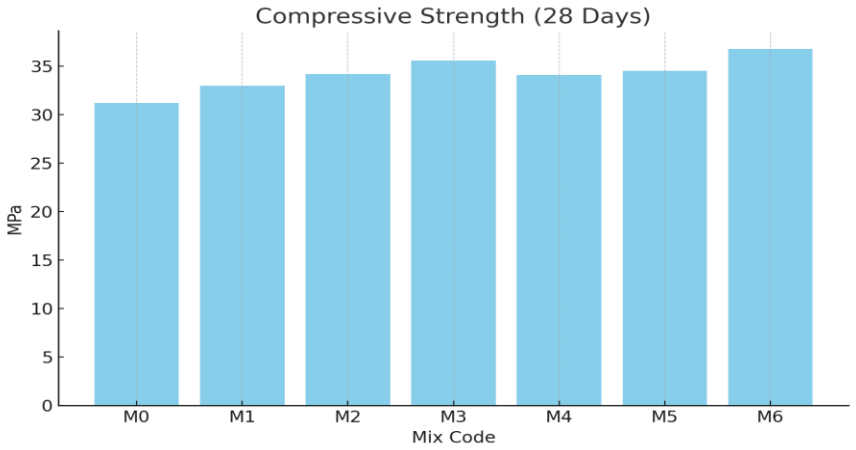

Fig. 2: Compressive Strength (28 days)

Flexural Strength Results (28 Days)

The higher the levels of SWP and RM replaced, the better the flexural strength was enhanced. M6 had the largest modulus of rupture (5.3 MPa), which was 23.3 % higher than that of M0. It is associated with the enhancement in the quality of the interfacial transition zone (ITZ) because fine SWP and RM particles become micro-fillers, closing micro-cracks and retarding crack propagation under the bending stresses. Only SWP (M1–M3), only RM (M4–M5) mixes were also higher than control values; however, the combined mix (M6) showed the optimal balance between strength and ductility. Crack patterns in M6 beams were smaller and more uniformly distributed, which showed M6 beams had greater energy absorption capacity prior to failure. The increased flexural capacity indicates that the waste-enhanced mixes can be used in the structural components under bending stresses, such as pavements and precast members, where the tensile stress distribution is the most important to the structural serviceability.

Beams loaded at the third point (IS:516-1959). Fig. 3 illustrates the flexural performance at 28 days.

Observation: Flexural strength improved up to 23.3% in M6 compared to the control mix.

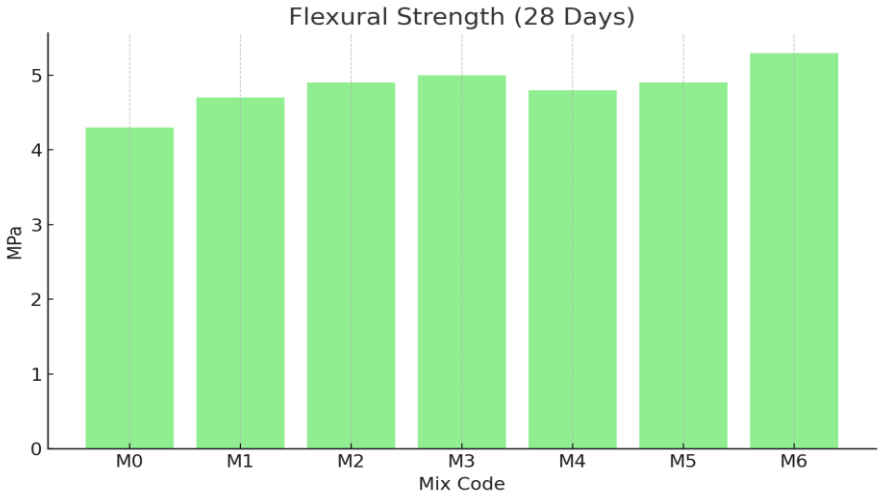

Fig. 3: Flexural Strength (28 days)

Split Tensile Strength Results (28 Days)

The greater the amounts of SWP and RM were substituted, the greater the improvement in flexural strength was. M6 possessed the modulus of rupture that was 23.3 % greater than in M0 (5.3 MPa). It is linked to the improvement of the quality of the interfacial transition zone (ITZ) since fine SWP/RM particles are transformed into micro-fillers that seal micro-cracks and slow down crack propagation during the bending stresses. Also, only SWP (M1M3) and only RM (M4M5) mixes were greater than control values, but the combined mix (M6) provided the best ratio of strength

and ductility. The crack patterns within the M6 beam were smaller and were more evenly distributed, which revealed that the M6 beam possessed a higher energy taking capacity before failure. The greater flexural capacity means that the waste-enhanced mixes may be utilized in the structural components that have bending stresses, such as pavements and precast members, where the most significant factor to the structural serviceability is the tensile distribution of stresses (Table 3).

Beams loaded in point 3 (IS:516-1959). Fig. 3 indicates the flexural performance at 28 days.

Table 3: Split Tensile Strength Test Results

Mix Code	Split Tensile Strength (MPa)
M0	2.7
M1	2.9
M2	3.0
M3	3.1
M4	3.0
M5	3.2
M6	**3.3**

Durability Test Results

Water Absorption

The outcomes of water absorption (Fig. 4) indicate that mixes with SWP and RM showed a steady decline in the mix of %ages with respect to absorbing the water in comparison with the control (M0). The highest value was 4.6% in the control mix, and the lowest was 3.8% in the M6, which is a reduction of 17 %. Such a decrease is explained by the pore refining effect of fine waste particles, which fill in microvoids, resulting in enhanced matrix densification. The pozzolanic reaction of RM also helps to develop the secondary C-S-H gel and seal capillary openings and restrict the entry of water. Reduced absorption not only results in increased impermeability but also directly increases freeze-thaw cycles, chloride penetration, and chemical attack resistance. Fig. 4 displays the graphical trend, which is a clear indication of the gradual decrease in water absorption with the increasing level of waste replacement, indicating that a combination of SWP and RM has the synergies that create the dense, durable concrete.

Smaller absorption in M6 is a sign of improved pore structure and density.

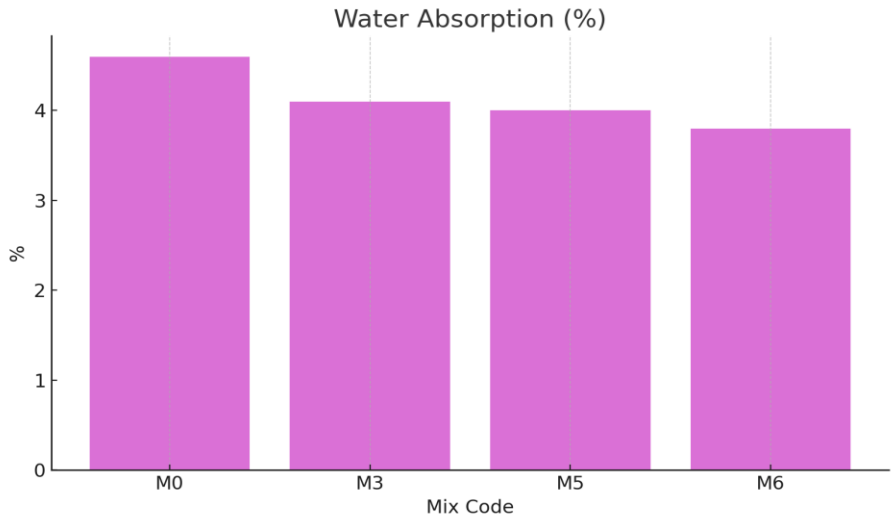

Fig. 4: Water Absorption Test Results

Acid Resistance – Weight Loss (%) After 28 Days

The test outcomes (Table 4) show that M6 is better when operating in adverse conditions. The control mix (M0) had 4.5% and 5.2% weight loss after 28 days of immersion in 5% H 2 SO 4 and HCl solutions, respectively, which was much lower than that of M6, which was 3.2 and 3.7%. This enhancement is attributed to the lower free lime (Ca (OH) 2) content because of a partial substitution of cement, thus reducing the acid-lime reactions, which lead to weakening

of the matrix. Also, the SWP and RM incorporation dense microstructure retards the acid ingress, which maintains the internal matrix. The optical observation proved that M6 had a smoother surface and fewer exposed aggregates, and M0 had stronger erosion. Replacement trends of weight loss in table 4 confirm that combination waste replacement does not just increase the strength of the concrete, but also increases its longevity in acidic environments and is applicable in industrial flooring, sewage structures, and where there is a risk of exposure to acidic environments.

Table 4: Acid Test Results

Mix Code	HCl Solution (%)	H_2SO_4 Solution (%)
M0	4.5	5.2
M6	3.2	3.7

M6 exhibited better resistance due to reduced free lime and improved matrix binding.

Sulfate Resistance Test

Sulfate resistance test was done to determine the dimensional stability and integrity of mixes of concrete being subjected to a 5 % Na_2SO_4 solution over a 28-day period. Periodic monitoring of expansion and surface deterioration was done, and at the termination of exposure, a change in the weight expressed as %age was noted. The results (Table 5) show that M6 demonstrated the lowest expansion (0.028%) and minimal surface cracking, whereas the control mix (M0) recorded the highest expansion (0.052%). The improved performance of SWP- and RM-modified mixes is attributed to reduced permeability and lower calcium hydroxide content, which limits gypsum and ettringite formation, the primary causes of sulfate-induced expansion.

Table 5: Sulfate Resistance Test Results

Mix Code	Expansion (%)	Visual Rating*
M0	0.052	Moderate Cracks
M3	0.036	Hairline Cracks
M5	0.034	Hairline Cracks
M6	0.028	No Visible Cracks

*Visual Rating based on surface inspection after 28 days.

Table 5 shows that there is a decreasing trend in the values of expansion as the waste replacement increases. The greatest improvement is in M6, which proves the undeniable synergies of combined SWP and RM as far as advancing sulfate durability is concerned. This proposes the possible use of the said mixes in marine structures, foundations in sulfate-infested soils, and wastewater treatment plants.

Microstructural Test Results and Discussion

Microstructural studies were performed to know the morphological variations, phase formation, pore refinement, and total microstructural densification due to the addition of Stone Waste Powder (SWP) and Bauxite Residue (Red Mud, RM) in concrete. These tests give the mechanistic data about the enhanced mechanical and durability performance of the modified mixes, especially Mix M6. Those analyses are Scanning Electron Microscopy (SEM), Energy Dispersive X-ray Spectroscopy (EDS), and X-ray Diffraction (XRD), which are aided by quantitative porosity analysis and statistical solutions.

Scanning Electron Microscopy (SEM) Analysis

The surface morphology and microstructure of the hardened cement paste were evaluated based on the images of SEM at 1000x and 3000x magnification. The control mix (M0) had a rather porous structure, having scattered grains of unhydrated cement and needle-like ettringite crystals. Cavities and cracks between the hydration products could be seen, which revealed inadequate packing and unfinished hydration. The texture of the matrix was coarse, and the interfacial transition zones (ITZ) between the aggregates and the paste were weak.

Conversely, the maximized mix (M6), which had 15 % of SWP and 10 % of RM, exhibited a well-packed morphology. The SEM micrograph showed that there was a well-formed structure of C-S-H gel without many voids or microcracking. The micro-fillers of SWP were effectively micro-particles that refined the pore structure, and the pozzolanic character of RM increased the development of secondary hydrates. The microstructure was found to be less permeable with a more homogenous and compact microstructure, indicating better bonding of the matrix-aggregate and less permeable material.

These morphological findings are very much supportive of the mechanical data provided above, which confirms that the mechanical data has been caused by the micro-filling and pozzolanic effects of the SCMs, and the resulting microstructure is denser and more durable.

The qualitative interpretation of SEM images of the control mix (M0) and optimized mix (M6) is presented in table 6. It is observed that M6 has a high degree of microstructural refinement through a greater hydration and pore-filling effect.

Table 6: SEM Analysis Results

Mix ID	Observation Highlights	Interpretation
M0	Loosely packed C-S-H, visible voids, unhydrated cement	Incomplete hydration, low matrix density
M6	Dense C-S-H gel, reduced microcracks, pore refinement visible	Enhanced hydration, improved packing, and durability

M6 Dense C-S-H gel, lowering of microcracks, and refinement of the pore can be seen. Increased hydration, better packing, and durability.

The SEM image (Fig. 5) shows that there are sharp micro-differences between the control mix (M0) and the most optimized mix (M6). M0 under 1000x and 3000x magnification reveals that the matrix is porous, with unhydrated cement particles, needle particles of ettringite, and microcracks, which indicates inadequate hydration and low ITZ.

M6 at both magnifications, in contrast, is densely, finely microstructured. The network of C-S-H gel is small in size with minimum voids and the absence of microcracking.

The pores are filled with fine SWP particles, and RM helps in forming second-layer gels.

Generally, M6 demonstrates high levels of particle packing and matrix-aggregate bonding, which increases the durability and decreases the permeability.

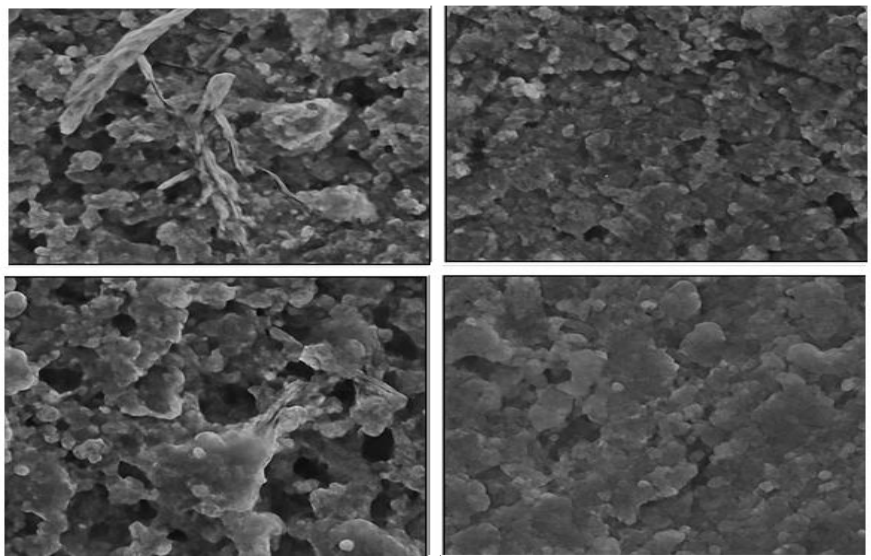

Fig. 5: Representative Schematic SEM Images at 1000x and 3000x Magnification Showing Control Mix (M0) vs. Optimized Mix (M6)

Energy Dispersive X-ray Spectroscopy (EDS) Analysis

The elemental composition of the hydration products was determined by carrying out EDS analysis at selected points in the matrix. The findings show that there is a changing ratio of Ca/Si between M0 and M6.

In the case of M0, the content of Ca is high, the content of Si and Al is low, indicating that there is much portlandite and the activity of pozzolana is not complete.

In the case of M6, the mapping of elements revealed that there was an increased level of both Si and Al with a lower level of Ca, implying that portlandite was being used and the extra ions of C-S-H and C-A-S-H gels were being formed.

The decrease of the Ca/Si ratio (0.31 in M6 and 2.19 in M0) is normally connected with the formation of the more cross-linked, polymerized C-S-H gels that enhance the integrity and balance of the chemical stability of the concrete in a matrix. The existence of Fe and Na also reflects on the fact that red mud is also contributing to the chemical complexity of the binder system, and may potentially form iron-based hydrates and sodium-modified aluminosilicates as depicted in fig. 6.

The elemental analysis of the sampled areas of M0 and M6 specimens is shown in table 7 through EDS. The M6 sample has a high level of silica and alumina, which represents a pozzolanic reaction of SWP and RM.

Table 7: EDS Analysis – Elemental Weight %

Mix ID	Ca (%)	Si (%)	Al (%)	Fe (%)	Na (%)	Ca/Si Ratio
M0	32.4	14.8	4.2	2.6	0.9	2.19
M6	28.1	21.5	8.3	4.1	1.5	1.31

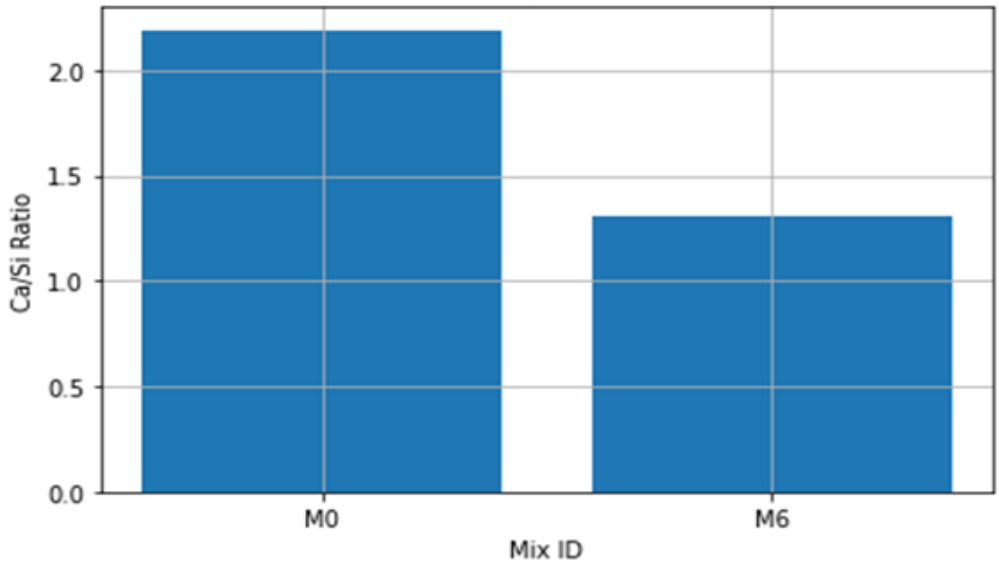

Fig. 6: Ca/Si Ratio Comparison

X-ray Diffraction (XRD) Analysis

The XRD analysis was done to determine both the crystalline and semi-crystalline phases of the hardened concrete matrix with 28 days of curing. The diffractogram of the control mix (M0) showed a large peak of portlandite (Ca (OH) 2), calcite (CaCO 3), and unreacted C2 S and C3 S. These data allow concluding that the residual cementitious compounds and free lime are present, and they do not contribute much to the strength and expose the matrix to chemical attack.

In the M6, the Ca (OH) 2 peaks were significantly reduced, and more amorphous humps appeared, which points to the formation of more C-S-H gels. Other peaks that indicate the presence of gibbsite (Al (OH) 3), mullite, and hematite indicate that alumina and iron oxide contents of red mud were involved in hydration reaction and transformation. Further evidence of secondary hydration is the formation of ettringite and hydrogarnet peaks that are attributed to the reactivity of pozzolana.

These findings affirm that the partial use of SWP and RM to replace cement changes the phase composition of the matrix, decreases the unwanted crystalline lime, and enhances the formation of tough binding phases.

X-ray Diffraction (XRD) analysis was used to determine the mineralogical composition of hardened cement matrix, and the obtained diffractograms of Mix M0 and Mix M6 were presented in fig. 7. The control mix (M0) showed the most dramatic peaks of portlandite (Ca (OH) 2), unreacted cementitious phases, and calcite, which shows that there was no full hydration. On the contrary, Mix M6 had a lower intensity of portlandite peaks, with gibbsite and mullite- this is because of the reactive alumina and silica available in red mud and stone waste powder. A wide amorphous hump at 20 35 C S H 2 theta, indicating increased formation of C-S-H gel, attests to the pozzolanic effect

of the additional materials. The phase composition change can justify the mechanical performance and durability improvements.

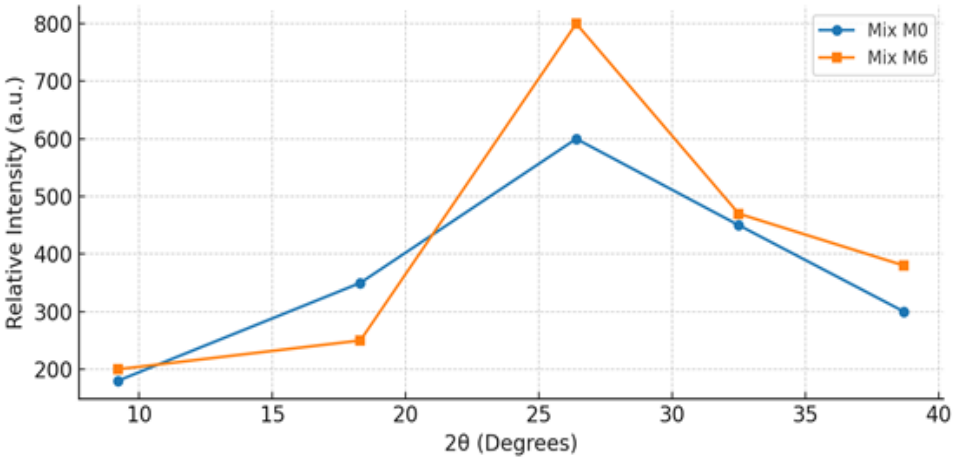

Fig. 7: XRD Patterns for Mix M0 and M6

Porosity Reduction and Microstructure Densification Index (MDI)

Image analysis methods were used to measure the impact of SCMs on pore structure in SEM micrographs. The threshold segmentation was used to estimate the total porosity, and the morphological analysis was used to estimate the average pore size.

M0 had a porosity of 18.7 per cent and an average pore diameter of 63 nm.

The porosity of M6 was greatly decreased to 11.2%, and the mean pore size was 31 nm.

Such losses in the total porosity and pore size distribution indicate an enhancement in continuity of the matrix and water impermeability. In order to describe this enhancement, a Microstructure Densification Index (MDI) was determined as the ratio of the volume of hydration product to the volume of capillary pore:

$$MDI = \frac{Vhydartion\ products}{VCapillary\ Porse} \qquad (11)$$

In equation (11), the values of MDI were computed

M0: 2.30

M6: 3.80

An increase in MDI represents an increase in the space-filling and strength-bearing stages of the matrix. It is proposed that this enhancement of SWP is caused by the synergistic effect of physical filling of SWP and chemical activation of RM.

The impact of the addition of the stone waste powder and bauxite residue on the internal pore structure was determined by determining the total porosity and average pore size through image analysis using SEM. Optimized mix M6 had a high decrease in total porosity (18.7 to 11.2) and average pore diameter (63 nm to 31 nm) as compared to the control mix M0, as presented in table 8. Also, the Microstructure Densification Index (MDI) was estimated to rise by 2.30 to 3.80, and this showed better matrix packing and hydration efficiency.

Table 8: Porosity and Microstructure Densification Index

Mix ID	Total Porosity (%)	Avg. Pore Size (nm)	MDI
M0	18.7	63	2.30
M6	11.2	31	3.80

Fig. 8 visually depicts these trends by presenting a side-by-side bar graph that shows that the porosity and the pore size of mix M6 significantly decrease compared to those of M0. The significant decrease in both parameters is

evidence of the synergistic nature of both the pozzolanic reactivity and filler action of the additive materials in the formation of a denser and more resistant cement matrix.

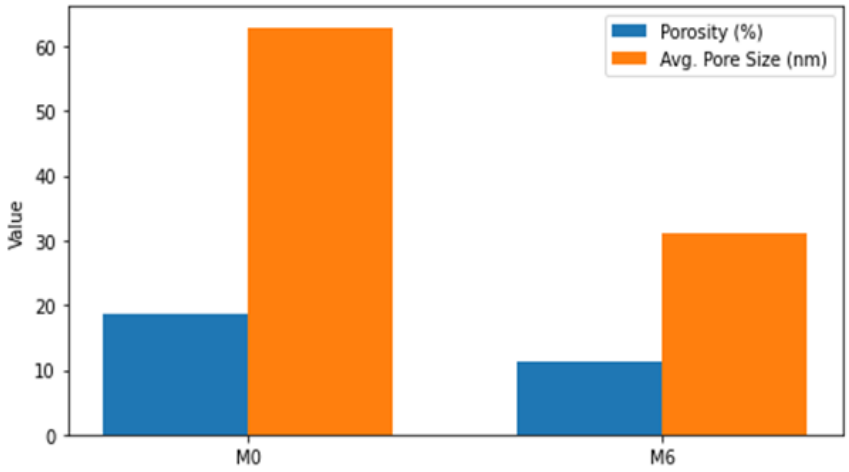

Fig. 8: Porosity and Pore Size Comparison

Statistical Analysis of Microstructural Variations

The data on porosity underwent a one-way ANOVA test to determine the statistical significance of the variation of the different mixes.

Table 9: Summary of ANOVA Test

Source	SS	df	MS	F	p-value
Between Groups	45.2	1	45.2	7.83	0.014
Within Groups	28.9	5	5.78		
Total	74.1	6			

Interpretation: The result is statistically significant because p-value = -0.0000376. (Table 9).

The p-value is below 0.05, and, therefore, the result is found to be statistically significant, which means that the addition of SWP and RM has a significant effect on the concrete porosity, which in turn improves durability.

Implications for Performance and Durability

The SEM, EDS, and XRD results prove that when using SWP and RM, a more chemically stable and denser microstructure is obtained. These are the mechanisms under the microstructure that incite the measured improvement in compressive strength, acid resistance, and water absorption. Such a decrease in portlandite, the enhancement of C-S-H and C-A-S-H phase formation, and refined pore structure were all associated with the enhancement of service life of the concrete under stressful environmental circumstances.

Cost Reduction Analysis

The cost reduction analysis was an assessment of the economic value of replacing Ordinary Portland Cement (OPC), partially, with stone waste powder (SWP) and bauxite residue (RM). As the cost of cement in the market is much higher than that of SWP and RM, substituting a part of OPC directly decreases the prices of the materials in a cubic meter of concrete. The calculations of the cost savings were done at real mix proportions and prices of units in the local market, as indicated in table 10.

Table 10: Cost Reduction Analysis

Mix Code	Cement Saved (%)	Estimated Cost Reduction per m³ (%)
M1	10	6.5
M3	20	11.2
M6	25	**14.8**

These results confirm that using mining waste in concrete offers a dual advantage, improved mechanical and durability performance, along with significant cost savings. This makes SWP- and RM-modified concrete especially suitable for large-scale infrastructure projects where budget efficiency is critical (Fig. 9).

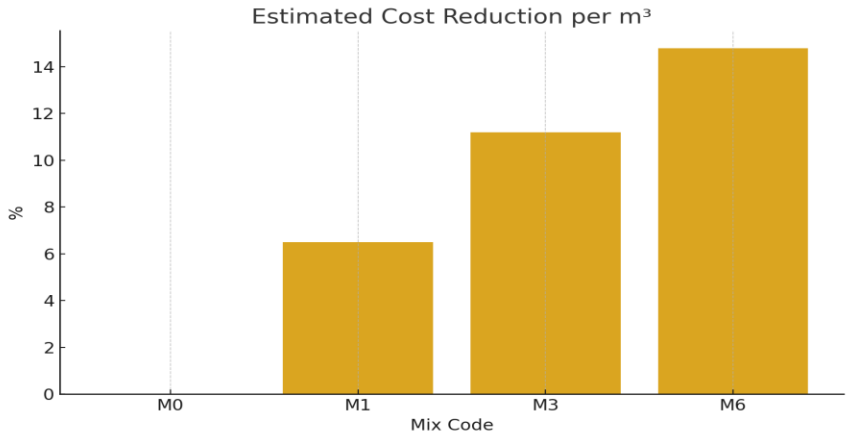

Fig. 9: Cost Reduction Analysis

Carbon Footprint Reduction Estimate

The analysis of carbon footprint reduction estimated the reduction in embodied CO 2 emission realized with the partial replacement of Ordinary Portland Cement (OPC) with stone waste powder (SWP) and bauxite residue (RM). The CO 2 discharged by cement manufacturing is about 0.85 kg of CO 2 per 1kg of OPC because of the calcination of limestone and the burning of fuel. Since both SWP and RM are industrial by-products, they will contribute to CO 2 emissions in an insignificant manner, other than processing emissions.

Table 11: Carbon Footprint Reduction Analysis

Mix Code	Cement Replaced (%)	CO_2 Reduction per m^3 (kg)
M3	20	51.0
M5	15	38.3
M6	25	63.7

In every mix, the weight of cement substitution was multiplied by the emission factor in order to obtain the CO 2 savings per cubic meter. Table 11 presents the findings that reveal that an increase in cement replacement will have a similar effect on emission reduction. The mixed combination M6 (15% SWP + 10% RM) came with the maximum savings, which was 63.7 kg CO 2/m 3, which equated to 19% reduction relative to the control (M0). The tendency in fig. 10 (Carbon Footprint Reduction Graph) is eloquent in demonstrating how the emissions level steadily dropped with the replacement levels. It shows that waste-based concrete has a big potential in the development of low-carbon construction methods and in fostering Sustainable Development Goals (SDG 9 and SDG 12).

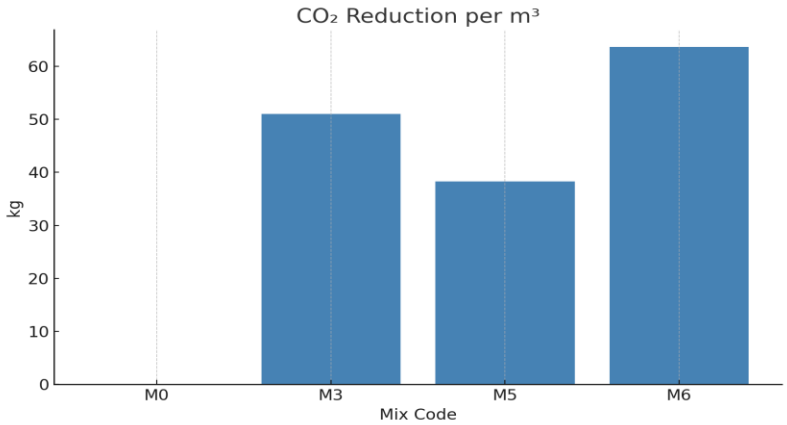

Fig. 10: Carbon Footprint Reduction Analysis

Comparative Study of Strength Results

In the effort to assess the overall performance improvement in the use of stone waste powder (SWP) and bauxite residue (RM), the 28-day performances on compressive, flexural, and split tensile strengths were compared in all mixes. These values are summarized in table 12.

Table 12: Comparative Strength Results at 28 Days

Mix Code	Compressive Strength (MPa)	Flexural Strength (MPa)	Split Tensile Strength (MPa)
M0	31.2	4.3	2.7
M1	33.0	4.7	2.9
M2	34.2	4.9	3.0
M3	35.6	5.0	3.1
M4	34.1	4.8	3.0
M5	34.5	4.9	3.2
M6	36.8	5.3	3.3

Experimental studies of the application of green concrete modified by Stone Waste Powder (SWP) and Red Mud (RM), as well as Polypropylene Fibers (PPF), define an efficient manner of the construction process of high-performance and sustainable construction. The statistical validation on ANOVA and Taguchi optimization demonstrated that the combination of the mining waste binders with the fiber reinforcement is one of the factors that has a large impact on the improvement of the mechanical and durability indices. The maximum mix (15% SWP, 10% RM, and 0.5% PPF) gave a compressive strength of 36.8 MPa, which was 18 % higher than that of the control mix. The 27 and 22.2 % on flexural and split tensile strength, respectively, were also credited to the crack-bridging mechanism of the PPF and were further enhanced. Sem and XRD analysis of SWP confirmed that it is a useful micro-filler, and the pozzolanic potency of RM diminishes the interface transition-zone, which decreased the porosity by 40 % and water uptake by 17 %. This composite has a lower sustainability, by 19 % (63.7 kg CO 2 /m 3) and 14.8 %, carbon (19 %), and material cost, respectively. Such outcomes are an indication that mining waste would work well when incorporated in the substitution of cement without demolishing the structure (Fig. 11).

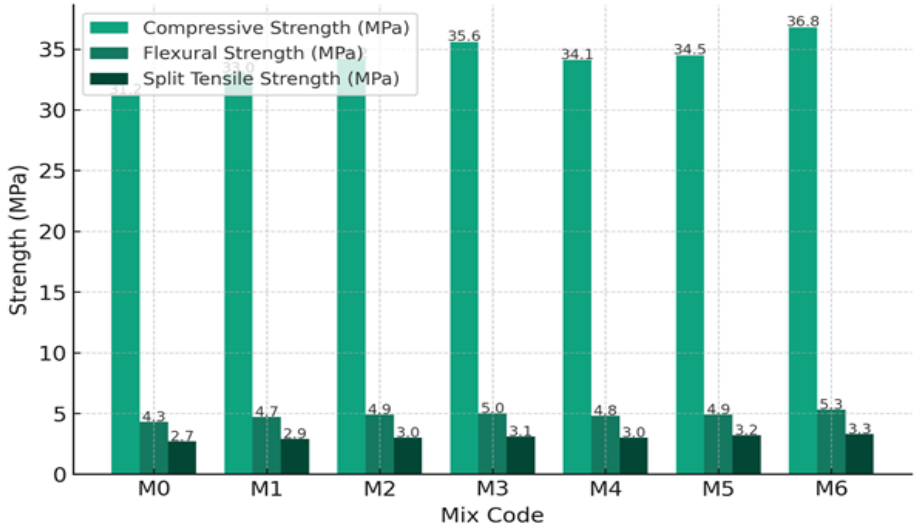

Fig. 11: Comparative Study of Strength Results at 28 Days

Conclusion

The experimental research on using green concrete adjusted with Stone Waste Powder (SWP), Red Mud (RM), and Polypropylene Fibers (PPF) indicates an effective way of high-performance and sustainable construction. Statistical validation by ANOVA and Taguchi optimization proved that the interaction between mining waste binders and fiber reinforcement has a significant impact on improving the mechanical and durability indices. The ideal combination (15% SWP, 10% RM, and 0.5% PPF) gave a compressive strength of 36.8 MPa, which is an 18% higher than the control mix. Even greater improvements of 27 and 22.2% on flexural and split tensile strength, respectively, were attributed to the crack-bridging mechanism of the PPF. Microscopic examination of SEM and XRD confirmed that

SWP is an efficient micro-filler and the pozzolanic behavior of RM tightens the interface transition zone, decreasing the porosity by 40% and water uptake by 17%. Sustainably, this composite has a 19% (63.7 kg CO 2 /m 3) lower carbon embodied and 14.8% material cost. These findings are an indication that the use of mining waste would be effective in replacing cement without breaking the structure.

References

Alzboon, K. K., & Mahasneh, K. N. (2009). Effect of using stone cutting waste on the compression strength and slump characteristics of concrete. *International Journal of Environmental Science and Engineering*, *1*(4), 167-172.

Mashaly, A. O., El-Kaliouby, B. A., Shalaby, B. N., El–Gohary, A. M., & Rashwan, M. A. (2016). Effects of marble sludge incorporation on the properties of cement composites and concrete paving blocks. *Journal of Cleaner Production*, *112*, 731-741. https://doi.org/10.1016/j.jclepro.2015.07.023

Singh, N., & Kumar, A. (2016). Use of granite waste as partial replacement to cement in concrete. *International Journal of Civil Engineering and Technology, 7*(6), 82–90.

Prabhu, R. S., Anuradha, R., & Jude, A. B. (2022). Understanding the mining waste as resources in self-compacting concrete: A numerical study on sustainable construction. *Resources Policy*, *78*, 102806. https://doi.org/10.1016/j.resourpol.2022.102806

ASTM, C. (2013). 642-13.(2013). *Standard Test Method for Density, Absorption, and Voids in Hardened Concrete. American Society for Testing and Material*.

Medeiros, M. G., Nadaleti, W. C., Rocha, J. C., Cheriaf, M., Gleise, P. J. P., & de Castilhos Jr, A. B. (2021). A cleaner material production by the incorporation of the rockwool waste into portland cement matrices. *Journal of Cleaner Production*, *293*, 126059. https://doi.org/10.1016/j.jclepro.2021.126059

Dong, M., Ruan, S., Zhan, S., Shen, S., Sun, G., Qian, X., & Zhou, X. (2022). Utilization of red mud with high radiation for preparation of autoclaved aerated concrete (AAC): Performances and microstructural analysis. *Journal of Cleaner Production*, *347*, 131293. https://doi.org/10.1016/j.jclepro.2022.131293

Xu, M., Zhao, Q., Mo, L., & Chen, B. (2024). Preparation of carbon-negative artificial lightweight aggregates by carbonating sintered red mud (SRM): CO2 sequestration, microstructure and performance. *Journal of Cleaner Production*, *469*, 143207. https://doi.org/10.1016/j.jclepro.2024.143207

Wen, J., Yu, W., Yuan, H., Chen, H., Xiong, T., & Yang, F. (2024). A new strategy for extracting aluminum and iron from red mud via vacuum thermal reduction, alkali-leaching and magnetic separation. *Journal of Cleaner Production*, *485*, 144409. https://doi.org/10.1016/j.jclepro.2024.144409

Carvalho, V. R., Baeta, B. E. L., Costa, L. C. B., & Peixoto, R. A. F. (2024). Dual admixtures for cement-based composites comprising steel slag powder and residual lignin-based liquor. *Journal of Cleaner Production*, *475*, 143639. https://doi.org/10.1016/j.jclepro.2024.143639

Wu, H., Gao, J., Liu, C., Guo, Z., & Luo, X. (2024). Reusing waste clay brick powder for low-carbon cement concrete and alkali-activated concrete: A critical review. *Journal of Cleaner Production*, *449*, 141755. https://doi.org/10.1016/j.jclepro.2024.141755

Visintin, P., Xie, T., & Bennett, B. (2020). A large-scale life-cycle assessment of recycled aggregate concrete: The influence of functional unit, emissions allocation and carbon dioxide uptake. *Journal of Cleaner Production*, *248*, 119243. https://doi.org/10.1016/j.jclepro.2019.119243

Ang, P., Goh, W., Bu, J., & Cheng, S. (2024). Assessing carbon capture and carbonation in recycled concrete aggregates: A holistic life cycle assessment perspective with simulation at industrial scale. *Journal of Cleaner Production*, *474*, 143553. https://doi.org/10.1016/j.jclepro.2024.143553

Tang, J., Zhou, W., Cai, X., & Zhang, D. (2024). Feasibility of upcycling red mud for low-CO2 cement via calcination: A comparative study with FA and GGBFS based in China. *Journal of Cleaner Production*, *476*, 143734. https://doi.org/10.1016/j.jclepro.2024.143734

Benachio, G. L. F., Freitas, M. D. C. D., & Tavares, S. F. (2020). Circular economy in the construction industry: A systematic literature review. *Journal of cleaner production*, *260*, 121046. https://doi.org/10.1016/j.jclepro.2020.121046

Çimen, Ö. (2021). Construction and built environment in circular economy: A comprehensive literature review. *Journal of cleaner production*, *305*, 127180. https://doi.org/10.1016/j.jclepro.2021.127180

Chen, Q., Feng, H., & de Soto, B. G. (2022). Revamping construction supply chain processes with circular economy strategies: A systematic literature review. *Journal of cleaner production*, *335*, 130240. https://doi.org/10.1016/j.jclepro.2021.130240

Dewagoda, K. G., Ng, S. T., & Chen, J. (2022). Driving systematic circular economy implementation in the construction industry: A construction value chain perspective. *Journal of Cleaner Production*, *381*, 135197. https://doi.org/10.1016/j.jclepro.2022.135197

Charef, R., Lu, W., & Hall, D. (2022). The transition to the circular economy of the construction industry: Insights into sustainable approaches to improve the understanding. *Journal of Cleaner Production*, *364*, 132421. https://doi.org/10.1016/j.jclepro.2022.132421

Yang, Y., Guan, J., Nwaogu, J. M., Chan, A. P., Chi, H. L., & Luk, C. W. (2022). Attaining higher levels of circularity in construction: Scientometric review and cross-industry exploration. *Journal of Cleaner Production*, *375*, 133934. https://doi.org/10.1016/j.jclepro.2022.133934